Simulation of auditory–neural transduction: Further studies

Ray Meddis
Department of Human Sciences, University of Technology, Loughborough LE11 3TU, England

(Received 31 July 1986; accepted for publication 3 November 1987)

A computational model of mechanical to neural transduction at the hair cell–auditory-nerve synapse is presented. It produces a stream of events (spikes) that are precisely located in time in response to an arbitrary stimulus and is intended for use as an input to automatic speech recognition systems as well as a contribution to the theory of the origin of auditory-nerve spike activity. The behavior of the model is compared to data from animal studies in the following tests: (a) rate-intensity functions for adapted and unadapted responding; (b) two-component short-term adaptation; (c) frequency-limited phase locking of events; (d) additivity of responding following stimulus-intensity increases and decreases; (e) recovery of spontaneous activity following stimulus offset; and (f) recovery of ability to respond to a second stimulus following offset of a first stimulus. The behavior of the model compares well with empirical data but discrepancies in tests (d) and (f) point to the need for further development. Additional functions that have been successfully simulated in previous tests include realistic interspike-interval histograms for silence and intense sinusoidal stimuli, realistic poststimulus period histograms at various intensities and nonmonotonic functions relating incremental and decremental responses to background stimulus intensity. The model is computationally convenient and well suited to use in automatic recognition devices that use models of the peripheral auditory system as input devices. It is particularly well suited to devices that require stimulus phase information to be preserved at low frequencies.

PACS numbers: 43.63.Bq, 43.63.Pd, 43.63.La

INTRODUCTION

Spike activity in auditory-nerve fibers is a probabilistic nonlinear function of the instantaneous amplitude of the acoustic stimulus. In recent years, a number of increasingly sophisticated computational models of this process have been presented that aim to explain the particular nonlinearities that occur at the junction between the inner hair cells and individual auditory-nerve fibers, the point of neuromechanical transduction (Siebert, 1965; Weiss, 1966; Nilsson, 1975; Schroeder and Hall, 1974; Oono and Sujaku, 1975; Eggermont, 1973; Geisler *et al.*, 1979; Brachman, 1980; Ross, 1982; Schwid and Geisler, 1982; Smith and Brachman, 1982; Westerman, 1985; Westerman and Smith, 1986; Cooke, 1986; Meddis, 1986).

These models are of interest to hearing researchers from a number of points of view. They offer a readily testable scientific explanation of the observed phenomena and stimulate the further development of theories of mechanism. Models that generate simulated spike trains in response to an acoustic stimulus are also a necessary prerequisite to detailed modeling of physiological processes occurring at "higher" levels of the system, for example, the cochlear nucleus or psychological processes such as auditory selective attention (e.g., Evans, 1986; Lyon, 1985). In addition, an immediate technological application of such spike-generating systems occurs in the design of automatic speech recognition devices. In hearing laboratories, spike generators are already in use for training researchers and testing apparatus without the need for live preparations.

Ideally, a proliferation of models should stimulate fruitful empirical studies by suggesting crucial experiments to decide between equally successful accounts. Regrettably, we have not yet reached that stage because no existing model has been shown to agree with all of the published results already available. Moreover, as new results are published, it is difficult to decide whether existing models can account for them except after a full-scale computational investigation. Armchair evaluation of the issue is normally totally inadequate. The purpose of this article is to report on a computational investigation of one model (Meddis, 1986) in the context of three recent research results: (a) the effect of stimulus amplitude on rapid and short-term adaptation time constants (Westerman and Smith, 1984); (b) the effect of increments and decrements of stimulus amplitude (Smith *et al.*, 1985); and (c) the recovery of rapid and short-term response capacity following masking stimuli (Westerman, 1985).

The article will also present an unintended, emergent property of the model which is the simulation of Rose *et al.*'s (1967) observation of phase-locked responding and its restriction to low-frequency acoustic stimuli. The high-frequency limit on phase locking is normally ascribed to low-pass filtering characteristics of the hair cell membrane as manifest in the decline of the ac/dc ratio of inner hair cell potentials as stimulus frequency rises (Sellick and Russell, 1980; Palmer and Russell, 1986). In the model, it arises as a consequence of delays in removing transmitter from the hair cell–nerve fiber junction.

I. THE MODEL

The model has been fully described elsewhere (Meddis, 1986; model B) but is summarized in Fig. 1. It can be fully

 0001-4966/88/031056-08$00.80

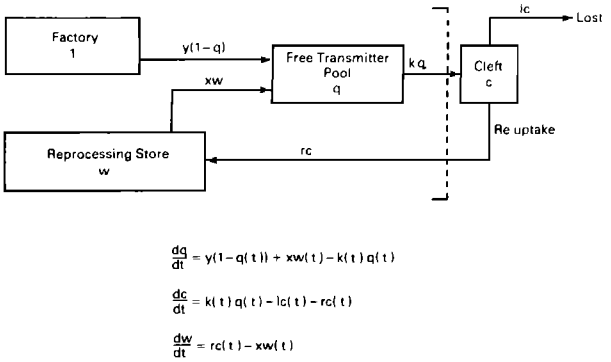

FIG. 1. Flow diagram for transmitter substance and differential equations defining the model. Taken from Meddis (1986), model B, Fig.10.

understood in terms of the production, movement, and dissipation of transmitter substance in the region of the hair cell–auditory-nerve fiber synapse. An amount $q(t)$ of transmitter exists inside the cell wall near the junction. A fraction $k(t)q(t)dt$ of this transmitter is released, between time t, and time $t + dt$ across the membrane into the cleft. A permeability factor $k(t)$ is a nonlinear function of the instantaneous amplitude of the signal after mechanical effects have been taken into account (although mechanical effects are ignored in this article),

$$k(t) = g[S(t) + A]/[S(t) + A + B], \quad \text{for } [s(t) + A] > 0,$$
$$k(t) = 0, \quad \text{for } [S(t) + A] \leqslant 0, \tag{1}$$

where A and B are parameters of the model and $S(t)$ is the instantaneous amplitude of the signal.

A fraction $lc(t)dt$ of the amount $c(t)$ of transmitter in the cleft is subject to chemical destruction or loss through diffusion. Another fraction $rc(t)dt$ is taken back up into the cell. The rest remains in the cleft to stimulate the postsynaptic membrane. It is assumed, for the sake of simplicity, that spike occurrence in the auditory nerve is linearly, probabilistically related to the residue of transmitter substance in the cleft. Accordingly, the quantity $c(t)$ is to be identified with the "excitation function" of Gaumond *et al.* (1983), Gaumond *et al.* (1982), or Gray's (1967) "recovered probability," i.e., the probability of spike emission disregarding refractory effects. Results below are expressed in terms of the excitation function because Westerman (1985) has presented the results of his observations in these terms and this method avoids the need to overlay the model's performance with additional, possibly controversial, assumptions concerning the recovery function of auditory-nerve activity.

Transmitter taken back into the cleft is not immediately available for release again but is delayed in a reprocessing store. A fraction $xw(t)dt$ of the amount of transmitter $w(t)$ in this store is continuously transferred to the free transmitter pool. The transmitter originates in a manufacturing base or "factory" that replenishes the free transmitter pool at a rate $y[m - q(t)]$, where m is the (approximate) maximum amount of transmitter to be found in the pool. In the unquantified version of the model, m is set to unity and all transmitter amounts are construed as fractions of the total possible amount.

The model is summarized by three differential equations that are given in Fig. 1. For the purposes of computation, dt is normally set to 0.00005 s except when explicitly stated. The three equations are evaluated; therefore, 20 000 times per second and the quantities $q(t)$, $c(t)$, and $w(t)$ are changed after each iteration. The model has seven parameters, y, x, l, r, g, A, and B, that can be set by the modeler (Table I).

II. METHODS OF EVALUATION

In a previous article (Meddis, 1986), it was shown that the model could realistically simulate mammalian adapted spike-rate/intensity function in the auditory nerve, appropriate interval and period histograms in response to sinusoidal stimulation, and suitable intensity related rate changes in response to increases and decreases in stimulus intensity. Subsequent research, to be described below, showed that the model could reproduce Smith's (1977) observation that the adaptation response following sudden stimulus increment is characterized by the sum of two exponential decay functions. It also indicated that the period histograms demonstrated a frequency-dependent phase-locking response that was analogous to Rose *et al.*'s (1967) observations.

These observations were followed by a period of parameter manipulation that aimed to fit the model's responding to detailed published numerical accounts of auditory fiber activity (Westerman and Smith, 1984). When a useful configuration of parameters had been established, the model was further tested against two recently published results involving the "additivity principle" and the effects of masking stimuli on the subsequent recovery of response capability. The following account is not a historical record of these developments but a demonstration of the strengths and weaknesses of the model using the final configuration of parameters. These values are given in Table I alongside the values used in Meddis (1986). Optimizing the configuration of parameters is a problematic affair with no guarantee of finding an ideal set of values. An account of the process of developing them will be postponed until after the exposition of the performance of the current model. Unless otherwise stated, the stimuli used to evaluate the model are 1-kHz sinusoidal

TABLE I. Values of parameters used in this and a previous evaluation of the model (Meddis, 1986).

	Meddis, 1986	New values
A	8	5
B	320	300
g	1 660	1 000
y	16.67	11.11
l	500	1 250
r	12 500	16 667
x	1 000	250
dt	0.00005	0.00005
	Time constants (ms)	
T_y	60	198
T_l	2	0.40
T_r	0.08	0.152
T_x	1	15.08

stimuli with either an instantaneous rise time or a rise time of 2.5 ms. The output of the model, its excitation function, is based on the cleft contents $c(t)$. The cleft contents are always averaged over one whole cycle of a 1-kHz signal then multiplied by a factor 69 080 in order to estimate the approximate firing rate in events (spikes) per second for that cycle. This value was based on fitting the functions by eye in Fig. 2 in order to arrive at a compromise, good fit between model results and empirical data.

A. Rate intensity

Using the parameters in Table I, column 2, a new set of rate-intensity curves was produced and is given in Fig. 2. The results are compared with Westerman and Smith's (1984) results for a single fiber (E8F2) with a center frequency of 1170 Hz. Figure 2 distinguishes two rate-intensity functions. The steady-state function represents the firing rate after adaptation to the stimulus tone and is sampled 300 ms after the tone onset. The onset function represents the firing rate in the 1-ms period with the highest rate of firing immediately following tone onset.

Westerman and Smith give 0 dB as "AV threshold." In the absence of a more precise definition, we have defined 0 dB for the model as the point at which the onset and steady-state functions diverge.

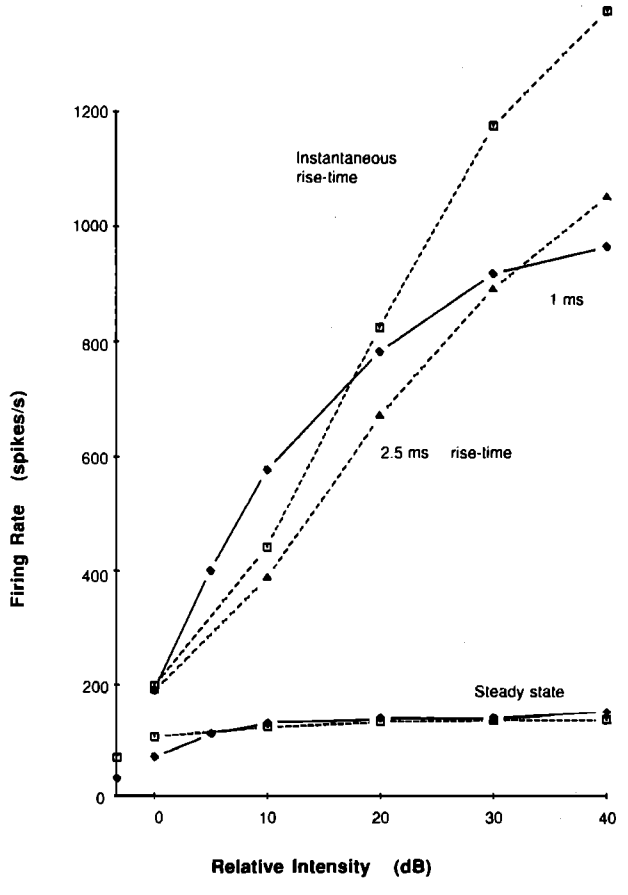

FIG. 2. Comparison of rate/intensity functions between model behavior (dotted) and Westerman's (1985, p. 74) gerbil data (solid line). In the case of the model, 1 ms (onset function) refers to the excitation function during the first (or highest) millisecond after tone onset. The steady-state function is based on the excitation function 300 ms after tone onset.

B. Rapid and short term adaptation

Westerman and Smith (1984) also studied the adaptation functions of fibers to brief tone bursts. Figure 3 shows a recovered PST histogram for the same fiber (E8F2) in response to tone bursts at 63 dB above threshold. Results of the model in response to the same stimuli are superimposed on their data.

Westerman and Smith characterized the adaptation function as the sum of two exponential decay functions plus a constant. The more rapid decline had a time constant less than 10 ms and the slower (short-term) decline had a very much slower time constant in the region of 70 ms. Figure 4 shows their estimate of the two time constants for the same fiber as a function of the intensity of the tone pulse. The short-term time constant remains steady across a 40-dB range. The rapid time constant, however, shows a steady decline from approximately 8 to 1.5 ms.

The results of the model (dotted line) are superimposed on the empirical values in Fig. 4. The method of fitting the exponentials to the model results is given in the Appendix. Because the model results take the form of smooth curves, the process of curved fitting is relatively straightforward. Time constants were the same for both instantaneous and 2.5-ms rise times.

C. Phase locking

From an early stage it was clear that the ability of the model's excitation function to reflect the fine structure of the stimulus was limited by the rate at which the transmitter could be cleared from the cleft. In the model this is affected by two routes: (a) dissipation and chemical destruction in the cleft and (b) reuptake into the cell. When these are slow relative to the stimulus frequency, phase locking will be less evident. The process will also be affected by the ability of the hair cell permeability function to respond quickly enough to

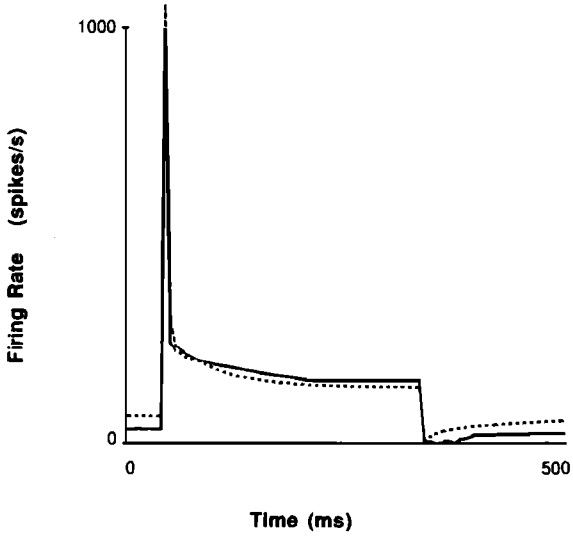

FIG. 3. Poststimulus time excitation function for the model (dotted line) compared to Westerman's (1985, p. 72) derived excitation function (solid line) for the same fiber used in Fig. 2. The stimulus for the model was a 43-dB, 300-ms, 1-kHz tone against a background of silence.

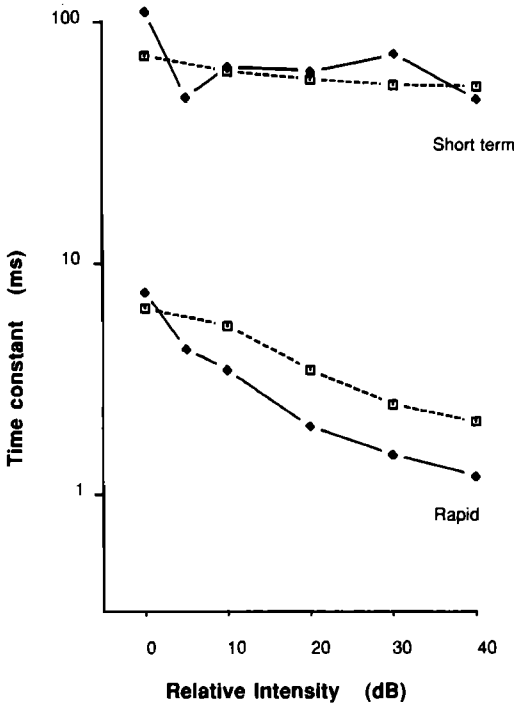

FIG. 4. Time constants for two additive exponential components fitted to the excitation function following brief tone bursts. The tone bursts for the model (dotted line) were 1-kHz sinusoids (2.5-ms rise time). The intensity of the tone bursts is relative to threshold. The empirical values (solid line) are taken from Westerman and Smith (1984, Fig. 8).

the instantaneous amplitude of the signal. This latter process is not simulated here so that the former process can be studied in isolation.

Figure 5 shows Rose *et al.*'s (1967) synchronization coefficient expressed as a function of stimulus frequency. This coefficient is based on period histograms and represents the "most populous" half of the histogram as a percentage of its total area. A value of 50% indicates no phase locking. A well-replicated finding is that synchronization measures decline in strength between 1 and 5 kHz.

To test the model, sinusoidal stimuli of 1, 2, 3, 4, and 5 kHz were used as stimuli and *dt* reduced to 0.01 ms. Figure 5 gives the synchronization coefficient for the computer simulation as a function of frequency.

Johnson (1980) also showed that, for a given frequency, synchronization increased with stimulus amplitude over a limited range. This range was not the same as the dynamic range of the adapted firing rate of the fiber but commenced its upswing well before the firing rate rises above the spontaneous level. The model successfully mimics this effect. Figure 6 shows both synchronization and rate measures derived from the model's performance as a function of stimulus amplitude.

D. Additivity test

The increase in firing rate following a stimulus amplitude increment has been shown to be independent of the state of adaptation of the fiber (Smith and Zwislocki, 1975; Smith, 1977; Smith *et al.*, 1985). This effect is true for onset (1-ms window) and short-term (10-ms window) measures of rate increase. The effect is also valid, following stimulus amplitude decrement, for short-term measures of rate decrease but not for onset rate measures. Following the method of Smith *et al.* (1985), a 1-kHz pedestal tone, 13 dB above threshold was presented to the model followed by a 6-dB increment or decrement at 0, 10, 20, and 30 ms after the onset of the pedestal. The increment/decrement in rate is the difference between the response to the pedestal plus increment and the pedestal alone.

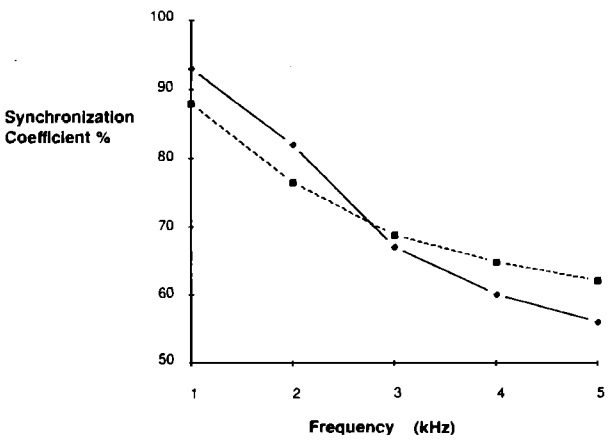

FIG. 5. Synchronization coefficient as a function of stimulus frequency. Model behavior (dotted line) was computed using $dt = 0.01$ ms. Empirical data (solid line) are taken from Rose *et al.* (1967).

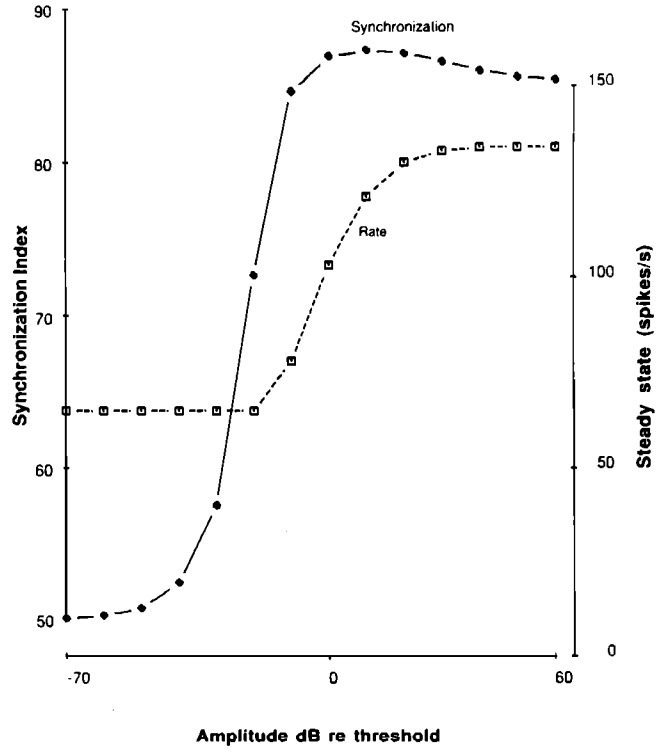

FIG. 6. Synchronization coefficient as a function of stimulus amplitude for a 1-kHz tone (solid line). Steady-state firing rate of the model as a function of amplitude for the same stimulus (dotted line).

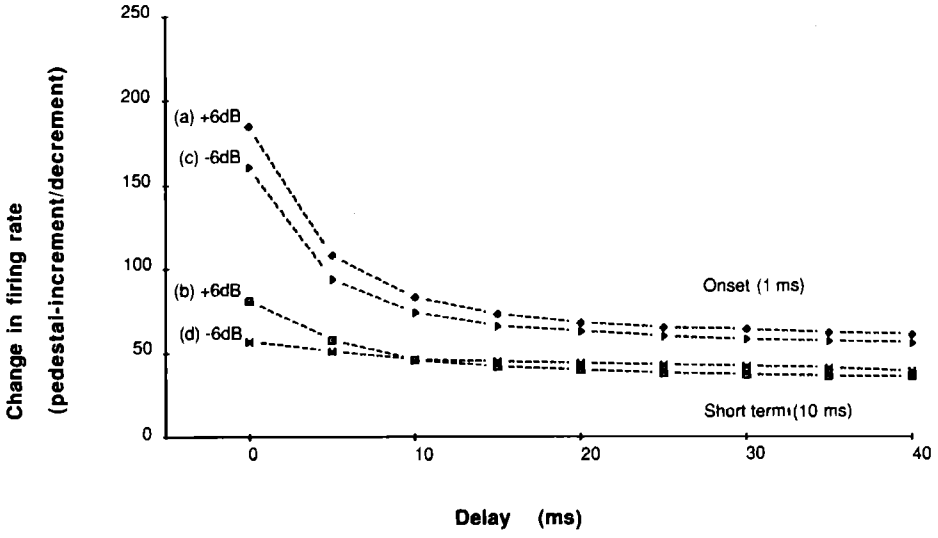

FIG. 7. Effects of prior adaptation on response to 6-dB increments and decrements of a 1-kHz pedestal tone presented at 13 dB above threshold. Here, (a) and (c) are rapid effects based on the first millisecond after stimulus change, and (b) and (d) are short-term effects derived from the first 10 ms after stimulus change. Empirical studies obtain horizontal lines for (a), (b), and (d).

The results do not agree with their results (Fig. 7). Their study showed horizontal functions for 6-dB increment (1- and 10-ms window) and for 6-dB decrement (10-ms window). The short-term decrement function (1-ms window) was shown to reduce with increasing delay. The model does show the required responses following stimulus decrements but is clearly discrepant during the first 10 ms of delay for stimulus increments.

E. Recovery of function

Following an intense masking tone, spontaneous firing of the fiber is briefly suppressed before slowly recovering to normal spontaneous levels. Westerman (1985) gives mean recovery time constants of 40 ms (standard deviation of 25 ms) based on 12 fibers. The model, using the specified final parameters, has a recovery time constant of 46 ms.

In the first millisecond following stimulus offset (50 dB), the excitation function of the computer model falls to a value equivalent to a rate of 9 spikes/s. This contrasts with a period of total suppression that is commonly observed. The model is, therefore, unable to explain a total suppression of spike activity. Alternatively, we may be seeking an explanation of the dead period in the wrong place. The total post-stimulus suppression may reflect *postsynaptic* fatigue that is not represented in the model at all.

Westerman (1985) also measured recovery of the capacity to respond to a second stimulus by presenting 30-ms test tones at varying intervals after the cessation of a 300-ms duration masking tone. Both tones were 43 dB above threshold. The response was measured as a decrement when compared to the response in the absence of a preceding masking tone. The onset rate is based on the first millisecond after the test tone onset. The short-term response is based on the period 20–30 ms after the onset of the test tone. Westerman's results are given as solid lines in Fig. 8. The use of a logarithmic scale for the response decrement measure means that the two straight line functions obtained represent exponential recovery in both cases. Westerman found two recovery time constants, 49 ms for the onset response and 68 ms for the short-term response for this particular fiber (E27F13, $CF = 842$ Hz). Clearly, the ability to produce a brief response recovers more quickly than the ability to sustain that response.

The dashed lines in Fig. 8 show the results of applying this experimental paradigm to the model. There are some clear discrepancies between the model's behavior and the empirical data. However, the dashed lines are approximately straight for much of their length and, therefore, indicate an exponential improvement in the capacity to respond. Between 0 and 20 ms, there is an upturn in the model results

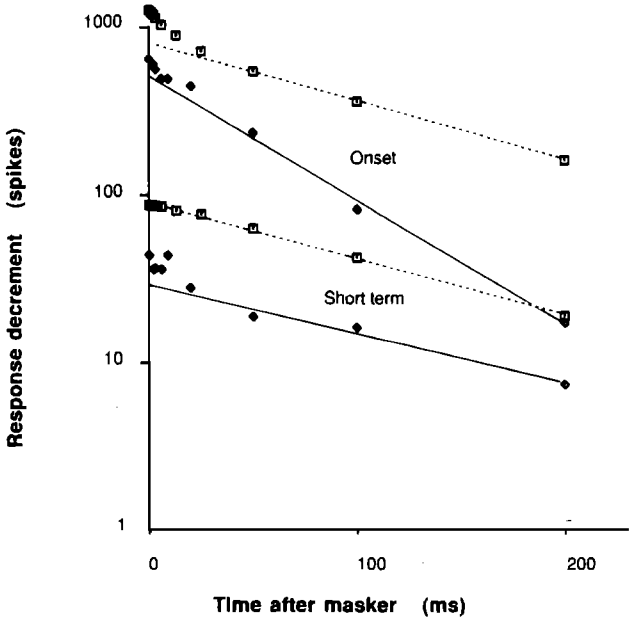

FIG. 8. Recovery of response following adaptation. The decrement is the difference between the response of an unadapted fiber to a 43-dB (*re*: threshold) 1-kHz tone and the response of a fiber soon after the offset of a 300-ms, 43-dB masking tone of the same frequency. The onset decrements are based on the maximal 1-ms firing rate after test tone onset. The short-term decrements are based on the rate between 10 and 30 ms after test tone onset. Solid lines are taken from Westerman (1985, p. 52, Fig. 21). Dotted lines represent the response of the model.

suggesting a departure from a simple exponential improvement. This is not necessarily inconsistent with Westerman's data points even though he chose to fit a single straight line throughout. I have redrawn his "best-fit lines" to illustrate this possibility. Perhaps a more detailed analysis of additional data will resolve this issue.

There are two important discrepancies that deserve attention. First, Westerman found different time constants for the recovery of onset and short-term responding. For seven fibers studied in detail, all had faster time constants for the recovery of the onset response. The model, by contrast, shows equivalent time constants for both recovery processes. For Fig. 8, Westerman gives time constants of 49 and 68 ms for onset and short-term functions. The time constant for both functions using the computer model was approximately the same as his short-term recovery function. For a sample of seven fibers, Westerman gives mean recovery functions of 48 ms (s.d. = 25 ms) for onset and 169 ms (s.d. = 79 ms) for short term.

III. OPTIMIZING PARAMETERS

The preceding exposition is based on simulations using an unchanging parameter set. Similarly, the rescaling of cleft contents to indicate potential firing rate used the same scale factor throughout. While it is encouraging that the model was able to fit the empirical data as well as it did, we have no guarantee that its performance could not have been improved with a better set of parameters. The method of parameter optimization used here was the laborious "hill-climbing" approach of changing one parameter at a time and noting the effect. If the effect was beneficial, this set of parameters was used as a new starting point; otherwise, it was necessary to revert to the previous set and make a different change.

The benefit of each new parameter change was assessed in terms in a number of dependent measures that compared model performance with target values derived from empirical data. The measures and the targets given in brackets are as follows: (1) ratio of spontaneous to 100-dB adapted firing rate (0.2); (2) dynamic range (30 dB); (3) rapid adaptation time constant near threshold (8 ms); (4) rapid adaptation time constants at 40 dB (2 ms); (5) short-term adaptation time constant near threshold (75 ms); (6) short-term adaptation time constant at 100 dB (75 ms); (7) phase locking (values given by Rose *et al.*, 1967).

It was not possible to match all of the targets exactly and the parameter set used represents a judicious compromise. It is quite likely that this set could be improved upon.

It is not a simple matter to identify individual parameters of the model with the dependent measures used. If it were, then the discovery of an optimum parameter set would have been very much easier. Changing any one parameter in isolation typically affects all measures. However, individual parameters typically affect some measures more than others: A, which occurs in the permeability equation, affects the spontaneous firing rate and the response threshold; B affects everything except the adaptation time constants; g influences the rate of outflow of transmitter from the cell into the cleft and thus affects all firing rates and rapid adaptation time constants; y, the replenishment factor, affects spontaneous and adapted firing rates as well as the short-term adaptation time constant; r, the rate of return of transmitter from the cleft into the cell, affects phase locking and the short-term adaptation time constant; x, the rate of transmitter reprocessing, affects only the adaptation time constants; l, the rate of loss of transmitter from the cleft—and, hence, from the whole system—influences all firing rates and the short-term adaptation time constant.

IV. DISCUSSION

Two possible uses of hair cell models were identified in the Introduction. First, they are a readily testable structural account of what is actually happening at the hair cell–auditory-nerve synapse. Second, they can be used as a generator of trains of spikes to act as input to other models of, for example, cochlear nucleus functioning, binaural hearing, selective attention, speech recognition, etc. Different criteria of usefulness apply in these various cases. Certainly, weaker criteria must apply to the model as an input device to other models because the development of theories concerning "higher" processes cannot wait until all the problems of characterizing the "lower" processes have been solved. Compromise is unavoidable.

The current model is clearly very suitable for use as a spike generator because the cleft contents, when multiplied by a suitable constant, can be viewed as a statement of the probability that a spike will occur at that time. A random number generator can, therefore, be used to decide whether a spike does occur at that time. The model will accept an arbitrary stimulus sampled at any rate that would normally be acceptable in acoustic analysis. In response, it produces a stream of spikes precisely located in time. Rate measures can be derived from this output, as required. More importantly, knowing the precise timing of each event is a special virtue for those analysis systems that depend upon the time intervals between spikes (e.g., Moore, 1982) or, more generally, which involve any kind of phase sensitivity (Patterson, 1987). The simplicity of the model allows for rapid numerical evaluation. A recent implementation on an 8-bit 6502 (1-MHz) processor runs at 10 times real time when using a 20-kHz sampling rate and we expect to produce a real-time implementation using a more powerful processor in the near future. Moreover, the model appears to mimic all of the major properties of auditory-nerve response. Such defects as have been revealed so far are unlikely to affect adversely research progress for systems using this model as an input device.

The failings of the model, however, are much more critical when evaluating its potential as a structural account of events taking place at the point where the auditory nerve meets the hair cell. It is not possible to make a direct comparison with other published accounts because this is the first time that this particular set of experimental paradigms has been simulated as a complete set. However, the range of phenomena successfully simulated suggests that the model defects are relatively minor. These involve two anomalies. First, the onset response shows an unrealistic sensitivity to level of adaptation during the first 10 ms of the adaptation

process. Second, recovery of the ability to respond to a new stimulus following an intense masking stimulus shows important discrepancies with empirical results.

The failure to replicate the additivity effect for onset responses is an important problem. A number of existing models (Schwid and Geisler, 1982; Smith and Brachman, 1982; Cooke, 1986; Westerman and Smith, 1986) have explicitly directed their modeling efforts towards explaining additivity by suggesting that stimulus intensity modulates the amount of transmitter eligible for release, i.e., the stimulus controls the *volume* of the free-transmitter reservoir. Westerman and Smith's (1986) most recent account proposes that both the volume *and* the membrane permeability are stimulus dependent. If these models in an explicit simulation can be shown to reproduce the additivity effects in the paradigm illustrated above, a case could be made for introducing multiple release sites or variable volume reservoirs into the model currently under discussion.

The attempt to simulate Westerman's (1985) function for the recovery of the ability to respond to a stimulus after previous intense stimulation also revealed discrepancies. In addition, Westerman (1985) finds two different exponential recovery functions, one for effects measured immediately after the onset of the test stimulus and one for the increase measured during a period 10–30 ms afterwards. For the bulk of the recovery period the model generates only one rate of recovery that is the same for both measures. Westerman and Smith (1986) have shown that this effect can be modeled by introducing an additional transmitter reservoir between the global store (factory) and the free-transmitter pool. Ross (1982) used two additional reservoirs in cascade. Some such amendment to the model may be required if it is not found possible to solve the problem by parameter manipulation.

One problem with the current position is that Westerman gives mean time constants of 48 and 169 ms for rapid and short-term effects, respectively. However, the standard deviations for these time constants are very high indeed (25 and 79 ms). Some rapid recovery time constants for certain animals must be slower than some short-term time constants for other animals. Moreover, some short-term time constants, in excess of 350 ms, appear to have been estimated over only 200-ms time periods. Insofar as there may be room for reevaluating Westerman's pioneering findings, it may be wise to delay radical revision of the computer model.

Having dwelt at length on the difficulties with the model, it is useful to rehearse the many phenomena that the model has successfully simulated. This summary is also drawn from a previous report (Meddis, 1986) that used the same model with only parameter changes. Phenomena successfully simulated are as follows: (1) steady-state rate/intensity functions; (2) poststimulus period histograms at various levels of stimulus intensity; (3) interspike-interval histograms for silence and 70-dB, 1-kHz sinusoid; (4) nonmonotonic functions relating incremental and decremental responses to stimulation amplitude changes as a function of background stimulation intensity; (5) adaptation functions that can be described as the sum of two exponential decay functions; (6) realistic synchronization coefficients decaying as a function of frequency; (7) realistic effects caused by decrements in stimulation intensity as a function of adaptation level for both onset and short-term measures and for short-term measures after stimulus increment; and (8) realistic rate of recovery of spontaneous firing rates following intense stimulation.

An interesting feature of the model is its reliance on transmitter movement delays to generate the familiar property whereby phase locking is limited by stimulus frequency. Little attention has been given to this possibility which exists whether or not we accept the idea of transmitter reuptake into the hair cell. Even on a pure dissipation and destruction principle, there must be some delay in clearing transmitter from the cleft. Recent work on the close association between the receptor potentials of inner hair cells and phase-locking indices is troubled by two difficulties: First, direct extrapolation from receptor potential seems to underestimate phase-locking ability, and, second, that the great variation among species in phase-locking ability may impose too great a strain on the theory (Palmer and Russell, 1986). While the model's successful use of transmitter movement as a basis for generating the phenomenon does not grant it the status of a true explanation, it does require that this possibility be taken into account in future discussion of the matter.

The reuptake principle was originally adopted for reasons of computational expediency. However, a recent study (Siegel and Brownell, 1986) has shown that this process may indeed be at work. They offer evidence of membrane recycling at the inner hair cell synapse. Some of the membrane recovered from the cleft (presumably by a process of invagination) appears to be used in the formation of new synaptic vesicles. This provides circumstantial evidence, at least, that a fast route exists for the reuptake of large molecules from the cleft into the presynaptic region.

While the model has many interesting and satisfactory features, it is accepted that it may benefit from modifications based on other published models. Unfortunately, no direct comparison has yet been made that would allow a summary of the respective strengths of the different models. It is proposed that the set of tests described in this article could provide a minimum subset for comparative testing of all current models and a project to do this is currently planned. For such a comparison to be fully effective, some objective and preferably automatic method for optimizing the parameters in each model is clearly called for—especially for those models that do not allow for analytic solutions. This problem is under active discussion in many areas of scientific endeavor (Kirkpatrick *et al.*, 1983) and some of the proposed solutions will be actively explored in this context.

APPENDIX

The adaptation curve of the excitation function following a stimulus increment was described in terms of the equation

$$Y_t = a + be^{-t/T_1} + ce^{-t/T_2}, \quad \text{(A1)}$$

where Y_t is the excitation function at time t, e is the exponential constant, and a, b, c, T_1, and T_2 are values to be discovered by the method. To begin, we need to find a minimum value of Y ($Y_{\min}$), so that Y can be rescaled thus,

$$y = Y - Y_{\min}. \quad \text{(A2)}$$

Since we know that adaptation, for our purposes, is virtually complete after a quarter of a second, we can use a value not much smaller than the excitation function after 300 ms of adaptation have elapsed for $Y_{\min}$. Here, $Y_{\min}$ is also taken as our estimate of the parameter a.

We assume that the first time constant (T_1) is unlikely to be greater than 10 ms. As a result, we do not expect this first process to make much contribution to the function after 40 ms. We, therefore, compute T_2 on the basis of values between, say, 40 and 80 ms:

$$T_2 = (80 - 40)/[\ln(y_{40}) - \ln(y_{80})]$$

and

$$c = \exp[\ln(y_{40}) + 40/T_2].$$

If we now remove the asymptote and the effects of the slow adaptation from the original data,

$$y'_t = Y_t - a - ce^{-t/T_2},$$

we can find the parameters of the rapid adaptation function using the two data points at 1 and 2 ms:

$$T_1 = (2 - 1)/[\ln(y'_1) - \ln(y'_2)],$$

$$b = \exp[\ln(y'_1) + 1/T_1], \quad a = Y_{\min}.$$

This method is adequate when the functions are smooth and the basic model holds. If random variation affects the data, then the time constants T_1 and T_2 must be estimated over a range of values using least-squares methods. An alternative method and references to the literature are given by Westerman (1985, Appendix B).

Brachman, M. L. (1980). "Dynamic Response Characteristics of Single Auditory Nerve Fibers," Special Report ISR-S-19, Institute for Sensory Research, Syracuse University, Syracuse, New York 13210.

Cooke, M. P. (1986). "A Computer Model of Peripheral Auditory Processing," Speech Commun. 5, 261–281.

Eggermont, J. J. (1973). "Analogue Modelling of Cochlear Adaptation," Kybernetic 14, 117–126.

Evans, E. F. (1986). "Cochlear Nerve Fibre Temporal Discharge Patterns, Cochlear Frequency Selectivity and the Dominant Region for Pitch," in *Auditory Frequency Selectivity*, edited by B. C. J. Moore and R. D. Patterson (Plenum, New York).

Gaumond, R. P., Kim, D. O., and Molnar, C. E. (1983). "Response of Cochlear Nerve Fibers to Brief Stimuli: Role of Discharge History Effects," J. Acoust. Soc. Am. 74, 1392–1398.

Gaumond, R. P., Molnar, C. E., and Kim, D. O. (1982). "Stimulus and Recovery Dependence of Cat Cochlear Nerve Spike Discharge Probability," J. Neurophysiol. 48, 856–873.

Geisler, C. D., Sanh Le, and Schwid, J. (1979). "Further Studies on the Schroeder–Hall Hair-Cell Model," J. Acoust. Soc. Am. 65, 985–990.

Gray, P. R. (1967). "Conditional Probability Analyses of the Spike Activity of Single Neurons," Biophys. J. 7, 759–777.

Kirkpatrick, S., Gelatt, C. D., Jr., and Vicchi, M. P. (1983). "Optimization by Simulated Annealing," Science 220, 671–680.

Johnson, D. H. (1980). "The Relationship between Spike Rate and Synchrony in Responses of Auditory-Nerve Fibers to Single Tones," J. Acoust. Soc. Am. 68, 1115–1122.

Lyon, R. F. (1985). "Processing Speech with the Multi-Serial Signal Processor," IEEE ICASSP-85, 981–985.

Meddis, R. (1986). "Simulation of Mechanical to Neural Transduction in the Auditory Receptor," J. Acoust. Soc. Am. 79, 702–711.

Moore, B. C. J. (1982). *An Introduction to the Psychology of Hearing* (Academic, London).

Nilsson, H. G. (1975). "Model of Discharge Patterns of Units in the Cochlear Nucleus in Response to Steady State and Time-Varying Sounds," Biol. Cybernet. 20, 113–119.

Oono, Y., and Sujaku, Y. (1975). "A Model for Automatic Gain Control Observed in the Firings of Primary Auditory Neurons," Trans. Inst. Electron. Comm. Eng. Jpn. 58, 352–358.

Palmer, A. R., and Russell, I. J. (1986). "Phase-locking in the Cochlear Nerve of the Guinea Pig and Its Relation to the Receptor Potential of Inner Hair Cells," Hearing Res. 24, 1–15.

Patterson, R. D. (1987). "A Pulse Ribbon Model of Monaural Phase Perception," J. Acoust. Soc. Am. 82, 1560–1586.

Rose, J. E., Brugge, J. F., Anderson, D. J., and Hind, J. E. (1967). "Phase-locked Response to Low-Frequency Tones in Single Auditory Nerve Fibers of the Squirrel Monkey," J. Neurophysiol. 30, 767–793.

Ross, S. (1982). "A Model of the Hair Cell-Primary Fiber Complex," J. Acoust. Soc. Am. 71, 926–941.

Schroeder, M. R., and Hall, J. L. (1974). "Model for Mechanical to Neural Transduction in the Auditory Receptor," J. Acoust. Soc. Am. 55, 1055–1060.

Schwid, H. A., and Geisler, C. D. (1982). "Multiple Reservoir Model of Neurotransmitter Release by a Cochlear Inner Hair Cell," J. Acoust. Soc. Am. 72, 1435–1440.

Sellick, P. M., and Russell, I. J. (1980). "The Responses of Inner Hair Cells to Basilar Membrane Velocity during Low Frequency Auditory Stimulation in the Guinea Pig Cochlea," Hear. Res. 2, 439–446.

Siebert, M. W. (1965). "Some Implications of the Stochastic Behaviour of Primary Auditory Neurons," Kybernetic 2, 206–215.

Siegel, J. H., and Brownell, W. E. (1986). "Synaptic and Golgi Membrane Recycling in Cochlear Hair Cells," J. Neurocytol. 15, 311–328.

Smith, R. L. (1977). "Short Term Adaptation in Single Auditory Nerve Fibers: Some Poststimulatory Effects," J. Neurophysiol. 40, 1098–1112.

Smith, R. L., and Brachman, M. L. (1982). "Adaptation in Auditory Nerve Fibers: A Revised Model," Biol. Cybernet. 44, 107–120.

Smith, R. L., Brachman, M. L., and Frisina, R. D. (1985). "Sensitivity of Auditory Nerve Fibers to Changes in Intensity: A Dichotomy between Decrements and Increments," J. Acoust. Soc. Am. 78, 1310–1316.

Smith, R. L., and Zwislocki, J. J. (1975). "Short term Adaptation and Incremental Responses in Single Auditory-Nerve Fibers," Biol. Cybernet. 17, 169–182.

Weiss, T. F. (1966). "A Model of the Peripheral Auditory System," Kybernetic 3, 153–157.

Westerman, L. A. (1985). "Adaptation and Recovery of Auditory-Nerve Responses," Ph.D. thesis, Syracuse University, Syracuse, NY.

Westerman, L. A., and Smith, R. L. (1984). "Rapid and Short Term Adaptation in Auditory-Nerve Responses," Hear. Res. 15, 249–260.

Westerman, L. A., and Smith, R. L. (1986). "A Diffusion Model of the Transient Response of the Cochlear Inner Hair Cell Synapse," Manuscript.